

Cosmic ray e^+e^- spectrum excess and peak feature observed by the DAMPE experiment from dark matter

Hong-Bo Jin,^{1,2} Bin Yue*,^{1,2} Xin Zhang,^{1,2} and Xuelei Chen^{†1,2,3}

¹*Key Laboratory of Computational Astrophysics, National Astronomical Observatories, Chinese Academy of Sciences, 20A Datun Road, Chaoyang District, Beijing, 100012, China*

²*School of Astronomy and Space Science, University of Chinese Academy of Sciences*

³*Center of High Energy Physics, Peking University, Beijing 100871, China*

(Dated: December 4, 2017)

The Chinese satellite Wukong, also known as the Dark Matter Particle Explorer (DAMPE) experiment (DAMPE), has released its observation data of the cosmic ray (CR) electrons and positrons. The data shows an excess in the energy spectrum up to TeV energy, and possibly also a peak-like fine structure at 1.4 TeV. We investigate the scenario that the source of the excess come from the annihilation or decay of dark matter particles. We consider the W^+W^- channel and direct e^+e^- channel (model A), and the double $\tau^+\tau^-$ channel and direct e^+e^- channel (model B). We find that the annihilation or decay of dark matter particles in the galactic halo can give excellent fits to the broad excess. However, the annihilation cross section is of the order of $10^{-23}\text{cm}^3\text{s}^{-1}$, larger than required for obtaining the correct relic abundance when dark matter freeze out. We then study whether the narrow peak at 1.4 TeV could be explained by a nearby subhalo, which thanks to the smaller distance, could supply e^+e^- within a narrow energy range. We find that in order to produce a peak width less than the DAMPE energy bin width (0.2 TeV), the source must be located within $r < 0.6\text{kpc}$. Our global fit models do not produce the peak-like feature, instead at 1.4 TeV the spectrum show either a slope or a cliff-like feature. However, if less than optimal fit to the data is allowed, the peak-like feature could be generated. Furthermore, an excellent fit with peak could be obtained with model B if the background is rescaled. If the dark matter decay and annihilation rates are determined using the broad excess, we find that the halo is too heavy ($10^9 M_\odot$) in the decay model, while for annihilation model a steep profile is required to avoid having very heavy ones. The halo can be searched or constrained by γ -ray photons from the inverse Compton scattering of its electrons.

PACS numbers:

I. INTRODUCTION

According to recent astronomical observations, about 26% of the total cosmic density is made up by non-baryonic dark matter (DM), much more than the 4.7% baryonic matter we know of [1]. The DM plays a crucial role in large scale structure growth and galaxy formation, but its presence is only inferred from its gravitational effects, while its nature is still unknown. A simple and plausible conjecture is that the DM are made up of unknown particles, which are electromagnetically neutral but participate in weak interactions. Such DM particles may annihilate or decay into standard model particles. In the indirect search of weakly massive interacting particle (WIMP) dark matter, one looks for the signature of dark matter by observing γ -ray, energetic neutrino or charged cosmic ray (CR) particles as annihilation or decay products (for a review see e.g. [2]). As these are also produced by other astrophysical processes, which are not always well understood, it is necessary to look for distinct signatures from the dark matter annihilation/decay processes. In the case of cosmic ray, most CR particles follow

power law distributions, which could be nicely explained as the result of diffusive shock acceleration by supernovae remnants (SNR), followed by a complicated transportation process in the Galaxy [3]. On the other hand, the dark matter particle has a specific mass, so the energy of particles produced in dark matter annihilation or decay would be distributed in a particular energy range, which may produce an excess or deviation from the simple power law in the CR energy spectrum. In particular, if the dark matter particle could annihilate or decay directly to a pair of standard model particles, this may produce a narrow line feature, which would be a smoking gun signature of dark matter, as there is no other known mechanism to produce such narrow line feature in the multi-GeV energy range.

The cosmic ray electrons and positrons have been measured by a number of balloon or space-borne experiments. The HEAT[4], ATIC [5], PAMELA [6], Fermi [7, 8], and AMS-02 [9] have measured the electron and positron spectrum up to 2 TeV. An intriguing excess above a few tens GeV were found by these experiments, though the uncertainty remains large at the high energy end where the CR flux drops. In addition, the ground based HESS experiment observes the e^+e^- spectrum indirectly at higher energies [10]. From joint analysis of these experiment, a possible break in the energy spectrum was found around TeV scale, though in such analy-

*Co-first author

†Corresponding author

sis the systematic uncertainty is sizable [11, 12]. Such an excess could be generated by dark matter decay or annihilations, but to obtain a large excess, the dark matter annihilation rate must be higher than usually assumed for achieving the correct abundance during its freeze out in the Early Universe, or are from a relatively nearby source such as a subhalo [10, 13–19]. Alternatively, the excess could be produced by some energetic astrophysical processes such as pulsars which inject energetic positrons or electrons in the CR energy spectrum [20–24].

The DAMPE satellite has made a new measurement of the electron and positron spectrum (the electrons and positrons are not distinguishable in its observation). This satellite is designed to have low background contamination from the much greater proton component of the cosmic ray, and have high energy resolution so that sharp feature in the cosmic ray electron and positron spectrum would not be erased by energy resolution issue [25]. Recently, the DAMPE experiment has released their measurement from 25 GeV to 4.6 TeV [26]. Their energy spectrum is consistent but higher than those from the AMS-02. A break in the energy spectrum is indeed found at about 1 TeV, confirming the earlier result from HESS experiment, and provides a very precise measurement of CR electron positron energy spectrum at the TeV energy range. These results raises new interest on the dark matter contribution to the cosmic ray electron and positron spectrum.

In addition to the break, there is also a single peak feature at 1.4 TeV, with a statistical significance of $\sim 3\sigma$. We should take a cautionary note here: the number of actual events detected in this energy bin is only 93, while for the two adjacent bins the numbers are 74 and 33 respectively, so it is possible that the large peak is due to a statistical fluctuation. This would become more clear in the future as more data is accumulated. Nevertheless, the peak is very intriguing, because in sources of astrophysical origin, such as supernovae remnant or pulsar, it is not easy to generate particles with a single energy. So if the peak is real, it would be of great importance to the indirect dark matter search. Indeed, as we shall see below, even in the dark matter scenario it is not easy to produce a narrow peak in the charged particle spectrum, because the electrons and positrons produced in dark matter decay or annihilation will diffuse into broad energy distributions during their propagation. So to generate a narrow peak in the spectrum, the source must be located at a very small distance where the diffusion does not take long time. One such possibility is a dark matter subhalo which is accidentally located near the Solar system.

In this paper, we shall investigate the scenario that the dark matter annihilation or decay serve as possible source of the excess cosmic ray electron and positrons in light of the new DAMPE data. The paper is organized as follows: in Sec. II we describe our method for computing the CR electron positron spectrum. We introduce our method of computation in Sec. II. In Sec. III we present the results

from fitting the broad spectral excess with the galactic halo dark matter contribution. In Sec. IV, we study whether the peak feature at 1.4 TeV could be generated by a nearby subhalo. In Sec. V we investigate what is the required mass for such subhalos, and the constraint on the model from inverse Compton scattered photons and CR isotropy. We conclude in Sec. VI.

II. METHODS

The propagation of charged CR particles in the Galaxy can be described as a diffusion process, with interaction with other particles, and energy loss by radiation and collision, as well as re-acceleration in the turbulent magnetic field [27]. To quantitatively model this process, the GALPROP software package has been developed, which solves the propagation equation with a Crank-Nicholson implicit second-order scheme [28]. The primary electrons are mostly produced in supernova remnants (SNRs). Their injection spectrum is modeled as a simple power-law form, as is expected from the diffuse shock acceleration mechanism [29]. In the propagation models, the source item of the primary electrons is also often described as a broken power law spectrum multiplied by the assumed spatial distribution described in the cylindrical coordinate Strong and Moskalenko [28]. The density of CR electron source is modeled as an exponential disc. The secondary electrons and positrons are produced during collisions of CR nucleons (protons dominant) with the interstellar gas [30]. The distribution of the interstellar gas, which collide with CR particles and generate secondary particles, is derived from the observational data of H and CO, etc. [31, 32]. The CR propagation time can be constrained observationally by the ratio between primary particles and the secondary particles, such as the $\text{Be}^{10}/\text{Be}^9$ and B/C ratios in the cosmic ray. Alternatively, with the advent of high quality data from the AMS-02 experiment, the CR model parameters may also be determined solely from the proton [33] and B/C [34] data of AMS-02, as is demonstrated first in Ref. [35], which yield tighter constraints. In this paper, we shall also follow this approach.

If some CR particles are produced by dark matter annihilation or decay, their propagation process are the same, only the injection source distribution and energy spectrum differ. For DM annihilations, we model the source term as

$$q(\mathbf{r}, p) = \frac{\rho(\mathbf{r})^2}{2m_X^2} \langle \sigma v \rangle \sum_X \eta_X \frac{dN^{(X)}}{dp}, \quad (1)$$

where $\langle \sigma v \rangle$ is the velocity-averaged DM annihilation cross section multiplied by DM relative velocity (referred to as cross section), $\rho(\mathbf{r})$ is the DM energy density distribution function, and $dN^{(X)}/dp$ is the injection energy spectrum of antiprotons from DM annihilating into standard model (SM) final states through all possible intermediate states X with η_X the corresponding branching

fractions. Similarly, the source term for decay can be modeled as

$$q(\mathbf{r}, p) = \frac{\rho(\mathbf{r})}{m_\chi} \Gamma_\chi \sum_X \eta_X \frac{dN^{(X)}}{dp}, \quad (2)$$

where Γ_χ is the decay rate. The density profile $\rho(r)$ of the dark matter halos were derived in N-body simulation, such as NFW[36], Isothermal[37], and Moore[38]. In this paper we use the Einasto[39] profile to model the dark matter distribution. The energy spectrum of electrons and positrons of each channel is calculated by PYTHIA v8.175 [40]. The hadronic model interaction part of the code is also modified to improve the treatment of secondary particles [41].

In the dark matter particle annihilation or decay, the electrons and positrons can be produced directly, here we shall call this the e^+e^- channel. Note that the annihilation or decay may produce an e^+e^- pair, or in one annihilation/decay they may produce either an e^+ or an e^- plus other particles, but on the whole produce equal numbers of e^+ and e^- . For our investigation these differences do not matter, though in the former case the energy of the electron or positron would be exactly m_χ (annihilation) or $m_\chi/2$ (decay). In this case the primary energy spectrum of electrons and positrons is a very narrow peak, which is around $E_0 = m_\chi/2$ (decay) or $E_0 = m_\chi$ (annihilation) for the pair production. The electrons and positrons may also be produced by decay or annihilation into intermediate particles, such as the W^+W^- channel or $\tau^+\tau^-$ channel, which further decays to produce electrons and positrons. In these cases the energy spectrum is generally more broadly distributed. In this paper we shall consider (1) the direct production model e^+e^- , (2) the model A: W^+W^- , and (3) the model B: double $\tau^+\tau^-$ pairs. In previous analysis, it has been found that in fitting the broad spectrum excess measured by the AMS-02 experiment, the other channels usually do not yield as good fit as the ones listed above [41]. The branching ratio of e^+e^- channel to W^+W^- channel ($\tau^+\tau^-$ channel), f , is treated a free parameter to explore the favored final state.

According to their origins, we divide the CR electrons and positrons into three components : 1) an astrophysical background, this is the primary electrons from distant astrophysical sources and the secondary electrons and positrons generated when these primary electrons propagate in the space between sources and observers; 2) a diffuse dark matter component, including the electrons and positrons produced by the annihilation/decay of the dark matter particles in the galactic halo and distant subhalos, and the secondary electrons and positrons generated during their propagation; 3) a component from a nearby subhalo, which may accidentally to be located at a very close distance that it significantly alter the CR energy spectrum.

A. The broad spectrum

Precise measurements of CR electrons and positrons were reported by the AMS-02 experiment [42]. They found that in the measured flux of electrons plus positrons, the positron fraction reaches the maximum of 15.9% at 305 GeV [43]. There is a positron excess against the astrophysical background, which is usually interpreted as produced by either pulsars or dark matter annihilation/decay [35, 44–47].

If equal amount of positrons and electrons at the same energy are produced by the additional sources such as pulsars, dark matter annihilation/decay, then by subtracting the same amount of electrons as positrons from the total spectrum, one can obtain the contribution of the astrophysical primary electrons. In [48], the primary electron background is extracted from the AMS-02 experiment, and it indeed follows a power law spectrum as is expected for electrons of the astrophysical origin. This knowledge of primary electrons in turn helps us to improve the understanding of the additional sources.

In a recent work [41] (J17 hereafter), it is found that the CR electrons and positrons background as measured by AMS-02 agrees well with the prediction by a convection and re-acceleration diffusion (DCR) model using the CR protons, positrons and B/C data of the same experiment. Based on the two-peaks feature of the CR electrons and positrons background spectrum, they further pointed out that the positron excess in AMS-02 experiment could be interpreted by diffuse dark matter annihilation, and the most relevant channels are the W^+W^- (in the bosons and quarks) and double $\tau^+\tau^-$ (in the leptons) annihilation channels.

The dark matter profile is chosen as Einasto [39], which is described approximately by a power-law density distribution:

$$\rho(r) = \rho_\odot \exp \left[- \left(\frac{2}{\alpha_E} \right) \left(\frac{r^{\alpha_E} - r_\odot^{\alpha_E}}{r_s^{\alpha_E}} \right) \right], \quad (3)$$

with $\alpha_E \approx 0.17$ and $r_s \approx 20$ kpc. The local DM energy density is fixed at $\rho_\odot = 0.43 \text{ GeV cm}^{-3}$ [49]. In this model there is no nearby sources such as dark matter subhalos, and the CR electrons and positrons coming from the dark matter annihilation is a diffuse distribution in the Milky Way. The energy spectrum of electrons and positrons of each channel is calculated by PYTHIA v8.175 [40]. Then based on the above density profile, the final energy spectrum after propagation is obtained via the GALPROP [50].

In this paper, we use the spectrum template generate as J17 for the W^+W^- , $\tau^+\tau^-$ and e^+e^- channels respectively, as the theoretical models for the broad spectrum excess. We leave the normalizations and branching ratio as free parameters.

B. Nearby source

Even for the dark matter originated scenario, typically the observed cosmic ray electron and positron spectrum would still be a broad bump rather than a narrow peak. Charged particles move in curved trajectories in the stochastic interstellar magnetic field, so their transportation in the galactic scale can be described as a diffusion process. The TeV electrons and positrons also lose their energy rapidly by synchrotron radiation and inverse Compton scattering, with a life time of $10^5 \sim 10^6$ years. Even if the electrons and positrons are produced at a single energy by dark matter decay/annihilation, the peak would still be broadened quickly as they propagate through the space. For the electron and positron spectrum to retain a narrow peak, the source must be fairly close by, so that the peak is not greatly damped by energy loss or momentum space diffusion during the propagation.

The N-body simulations show that in the galactic dark matter halo there could be a large number of subhalos which were produced during the hierarchical structure formation process [51, 52]. Many of such halos did not form stars so they can not be observed directly (see Ref. [53] for a recent review). So below we compute the contribution to the electron and positron spectrum from a nearby subhalo, and see if the peak in the energy spectrum could be reproduced.

The CR spectrum from a nearby subhalo can be simulated with the GALPROP code. However, as the location and mass of such a subhalo is unknown, searching the parameter space with such simulation would be computationally expensive. Here, we consider an analytical solution of the CR diffusion equation from a nearby source. While this is not as accurate and comprehensive as the GALPROP code, for the nearby source it could provide a fast approximation.

We first assume the source produce electrons and positrons with a single energy E_0 , from a point source. The propagation equation of primary cosmic ray electrons (ignoring secondary ones produced in particle collision) can be written as

$$\begin{aligned} \frac{\partial \psi}{\partial t} = & \nabla \cdot (D_{xx} \nabla \psi - V_c \psi) + \frac{\partial}{\partial p} [p^2 D_{pp} \frac{\partial \psi}{\partial p}] \\ & - \frac{\partial}{\partial p} [\dot{p} \psi - \frac{p}{3} (\nabla \cdot V_c) \psi] + \mathbf{S} \end{aligned} \quad (4)$$

where $\psi(\mathbf{r}, p, t)$ is the number density of electrons per unit energy, D_{xx} and D_{pp} are the spatial and momentum diffusion coefficients respectively, V_c the bulk velocity, and \mathbf{S} the source distribution. For the present problem, $p \approx E$. This is a linear equation, so we may solve the subhalo contribution separately, and just adding it to the solution for the whole galaxy.

The diffusion coefficient and other parameters in the cosmic ray propagation model were fitted with other observations [54], $D_{xx} = D_0(\rho/\rho_0)^\delta$, where $D_0 = 6.59 \times 10^{28}$

$\text{cm}^2 \text{s}^{-1}$, $\rho = pc/Ze$ and $\rho_0 = 4 \times 10^3 \text{ MV}$, we take $\delta = 1/2$ here. We approximate the energy loss rate per electron $b \equiv |dE_e/dt|$ as constants. In the TeV energy range, the electrons and positrons lose their energy primarily by synchrotron radiation and inverse Compton scattering,

$$\begin{aligned} b &= \left(\frac{dE_e}{dt} \right)_{\text{syn}} + \left(\frac{dE_e}{dt} \right)_{\text{ICS}} \\ &\approx 5.8 \times 10^{-13} \text{ ergs}^{-1} = 3.6 \times 10^{-10} \text{ GeVs}^{-1}, \end{aligned} \quad (5)$$

at 1.4 TeV. Also, if the source is nearby, the diffusion in momentum space which is due re-acceleration can be neglected, as $\frac{D_{pp}}{E} \sim 2.9 \times 10^{-17} \text{ erg s}^{-1} \ll b$.

The dynamical time scale of the Milky Way is of order 10^8 year, so the time scale for the subhalo to pass by is much longer than the life time of the electron and positrons. We may then assume a steady state for the cosmic ray spectrum is reached, $\partial \psi / \partial t = 0$. We ignore the bulk velocity V_c , and approximate D_{xx} and b as constants. For a point source of monochromatic electron and positron injection, $\mathbf{S} = Q \delta(\mathbf{r}) \delta(E - E_0)$. then the propagation equation could be simplified as

$$D_{xx} \nabla^2 \psi - b \frac{\partial}{\partial E} \psi + Q \delta(r) \delta(E - E_0) = 0. \quad (6)$$

This equation can be solved by making a 3D Fourier transform over the spatial dimensions and a 1d Laplace transform over time. If the source is very nearby, we do not need to consider the global confinement to the galactic disk by the magnetic field. The solution in the spherically symmetric case is given by

$$\psi(E_0, E, r) = \frac{Q}{b} \frac{\exp[-\frac{r^2}{(4\pi D_{xx}/b)(E_0 - E)}]}{[(4\pi D_{xx}/b)(E_0 - E)]^{3/2}}. \quad (7)$$

The observed specific intensity of particles number flux is $J \approx \psi c / (4\pi)$.

If the injected electrons and positrons are not of a single energy but has an energy distribution of dN/dE , the corresponding spectrum could be obtained by

$$J = \frac{cf}{4\pi(1+f)} \int dE' \frac{dN}{dE'} G(E', E, r) \quad (8)$$

where the Green function $G(E', E, r)$ is given by Eq.(7). If the annihilation or decay has both direct e^+e^- channels and other channels, the result is given by the sum of all the channels.

We show the electrons and positrons spectrum produced via the different channels in Fig. 1, for model A (top panel) and model B (bottom panel). Here we fix $E_0 = 1.5 \text{ TeV}$ and $f = 0.01$. In each case we showed the result for $r = 1 \text{ kpc}$ and $r = 0.1 \text{ kpc}$. The total injection rate Q are adjusted ($Q = 10^{38}, 10^{41}$ for $r = 0.1, 1 \text{ kpc}$ respectively) so that the curves can be show on the same plot. The direct pair production spectrum are shown in both channels as solid lines. As we expected, the closer the source, the narrower the peak. For $r = 0.1 \text{ kpc}$ (blue)

the peak is very sharp, while for $r = 1\text{ kpc}$ (red) the peak is a much broader one. Compared with the direct production case, the electrons and positrons produced via the W^+W^- have broader distributions, as the electrons produced in this channel is not monochromatic. But again the peak is located at higher energy for the $r = 0.1\text{ kpc}$ (blue) case than the $r = 1\text{ kpc}$ (red) case. In the case of $\tau^+\tau^-$ channels, however, the peaks of the distribution are located at almost the same energy regardless of the distance, showing that in this case, the e^+e^- spectrum from decay or annihilation is already too broad that the distance almost does not matter. If we want to generate a peak in the spectrum, the direct e^+e^- channel have to be used, and to achieve the narrow peak with width less than 0.2 TeV , the source must be located within $r < 0.6\text{ kpc}$.

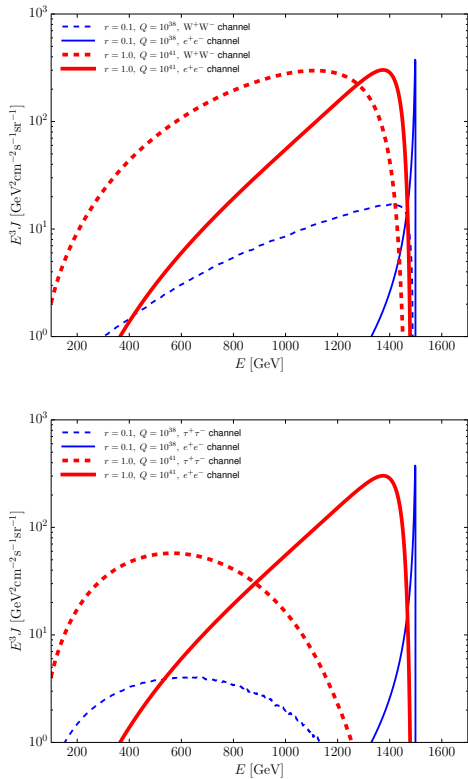


FIG. 1: The specific intensity of the electrons and positrons number flux from a nearby subhalo with different distances and different emission rate of annihilation/decay productions. Top panel is for model A while bottom panel is for model B.

We fit the normalization A of the broad spectrum electrons and positrons due to W^+W^- channel and the branching ratio f of the e^+e^- channel to the W^+W^- channel, the distance r , and the amount of injection Q from the statistics:

$$\chi^2(A, f, r, Q) = \sum \frac{[\langle J_i^{\text{nr}}(f, r, Q) \rangle + \langle J_i^c(A, f) \rangle - J_{\text{obs}}^i]^2}{\sigma_{\text{stat},i}^2 + \sigma_{\text{sys},i}^2}, \quad (9)$$

where $\langle J_i^{\text{nr}}(f, r, Q) \rangle$ is the mean intensity from the nearby source, including the W^+W^- channel and the e^+e^- channel in the i -th energy bin; while

$$J_i^c(A, f) = AJ_W^{\text{br}} + fAJ_e^{\text{br}} + J_{\text{bg}}, \quad (10)$$

the astrophysical background J_{bg} , the template the broad spectrum electrons and positrons due to DM annihilation/decay, including the W^+W^- channel, AJ_W^{br} , and e^+e^- channel, fAJ_e^{br} , are all generated using the algorithm presented in [41]. For simplicity we fix $E_0 = 1.5\text{ TeV}$. Adopting a different value within $\sim 0.1\text{ TeV}$ does not change our result.

III. FITTING WITH THE BROAD SPECTRUM

The CR electron spectrum has been measured by a number of experiments, such as the Veritas [55], HESS[56, 57] and Fermi-LAT[58] before the DAMPE data release. These observations indicate a remarkable break in the spectrum at TeV scale. However, the electron data from the ground based atmospheric Cherenkov telescopes such as HESS have large uncertainties from the subtraction of hadronic background and discrimination against gamma rays events[56]. In detail, the very-high-energy flux of HESS electrons is described by an exponentially cutoff power law with an index of 3.05 ± 0.02 and a cutoff at $2.1 \pm 0.3\text{ TeV}$ in the range of 700 GeV to 5 TeV [56]. The low-energy extension of the HESS electron measurement are from 340 GeV to 1.7 TeV with a break energy at about 1 TeV [57].

The TeV break of CR electrons are now confirmed by the highly precise DAMPE observation. If we assume the primary electron is described by a power law, while the excess electrons and positrons have the same spectral distribution, the degeneracy between the background and excess can be broken, and the origin of the TeV break is connected to the positron excess [59]. This is confirmed in [48], where the features of the primary electron spectrum is carefully studied, which showed a power law primary electron spectrum without TeV break.

Here, we derive the excess of electrons under the same assumption that the excess electrons and positrons are the same, and use the AMS-02 experiment data on positron fraction for subtraction [42]. We then compute the excess produced by dark matter particle annihilations in the galactic halo. We consider the annihilation to e^+e^- via the W^+W^- channel, and via the double $\tau^+\tau^-$ and e^+e^- channels.

In Fig. 2, we show dark matter annihilation model fit to the DAMPE measured spectrum data. We plot the primary electrons derived from AMS-02 $e^- - e^+$ data, the dark matter contribution, and the dark matter plus background total. The top two panels show the model A (W^+W^- channel) results, while the bottom two show the model B (double $\tau^+\tau^-$ and e^+e^- channels) results. We see all these models provide good fit to the data. The model A fit is better than model B in this case for much

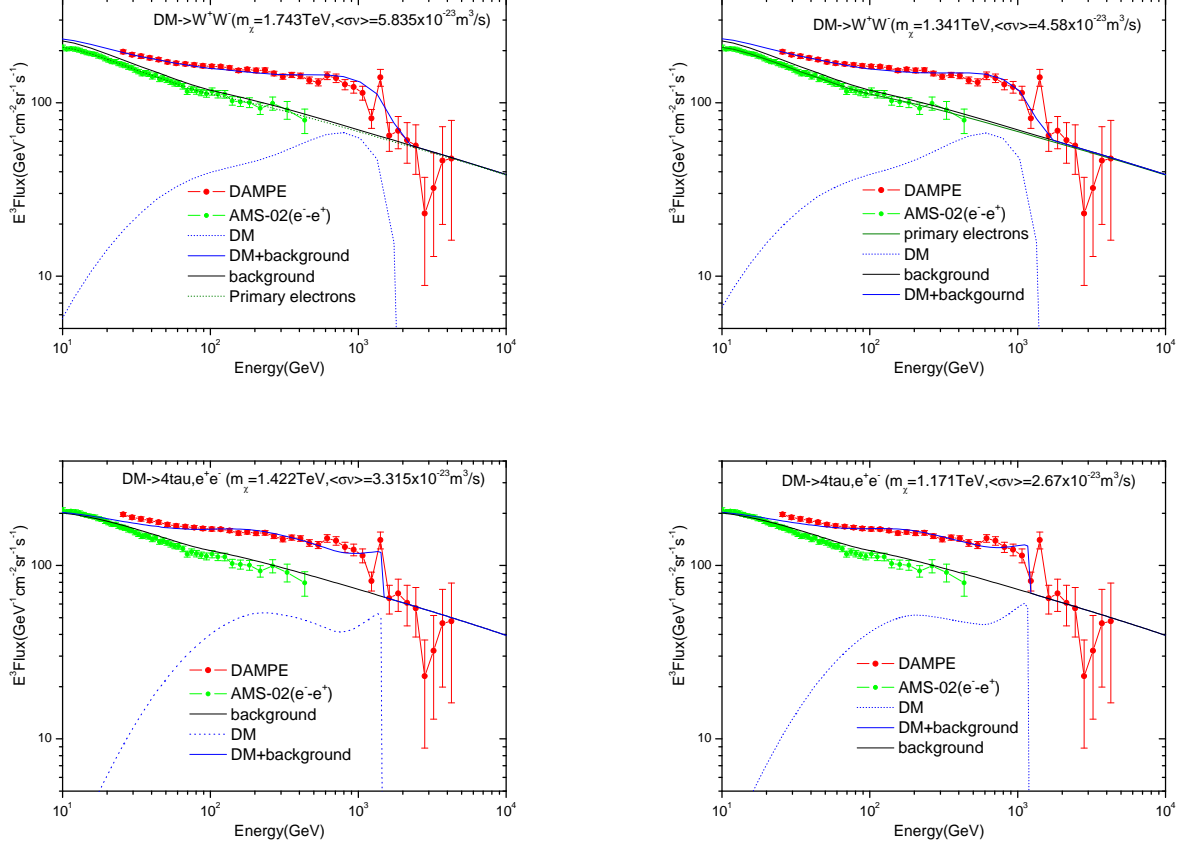


FIG. 2: The primary electrons background derived from $(e^- - e^+)$ of the AMS-02 data [43] and the total flux of CR electrons and positrons background measured by DAMPE. The curves that fit the data including and excluding the peak point near 1.4 TeV are shown in the left and right panel respectively. We write the minimum reduced χ^2 , best-fit DM particle mass m_χ and the velocity weighted cross-section $\langle\sigma v\rangle$ in each panel.

of the lower energy spectrum, its spectral shape agrees with the data very well.

In the left panels of Fig.2, we try to fit all data points including the peak point in the DAMPE data, while in the right panels we excluded the peak point. By excluding the peak point, the fit to the other points may be improved, as is the case of the W^+W^- channel. The double $\tau^+\tau^-$ and e^+e^- channels provide a way to fit the peak point. In this model there is steep drop of the spectrum at the dark matter mass, this cliff-like edge could be used to fit the peak point, though in this case the fit is worse for the energy just below 1.4 TeV.

The mass of the dark matter particle are 1.743 TeV and 1.341 TeV for model A, and 1.422 TeV and 1.171 TeV for model B. The required annihilation cross sections are typically $\sigma v \sim 10^{-23} \text{cm}^3 \text{s}^{-1}$, which is within the constraint derived from the AMS-02 electron data[44]. The cross section values are however larger than the one required to get correct abundance of WIMPs during the thermal decoupling. To obtain large abundance, the dark matter must be produced non-thermally in the early Universe,

or the cross section of its annihilation in the current time must be somehow enhanced [13, 14]. Moreover, while the cross section is derived for e^+e^- , we note that these are larger than the observational limits on annihilation cross section to photons derived from observations of the dwarf spheroidal galaxies[60, 61]. The required cross sections are one order of magnitude greater than those of VERITAS[60], and three order larger than the one from Fermi-LAT[61]. Although the γ -ray and e^+e^- cross sections could be different, we expect them to be of the same order, and special mechanism may be needed to achieve the large cross section to e^+e^- while not violating the γ -ray bound.

In the above we have discussed the case of annihilation. In the case of decay, except for the mass which is doubled and the rate is determined by decay life time instead of the annihilation cross section, many things are similar. In principle, the dark matter annihilation and decay results may differ, because the annihilation rate $\propto n^2$, while the decay rate $\propto n$, where n is the number density of the dark matter particle, so the source distribution is

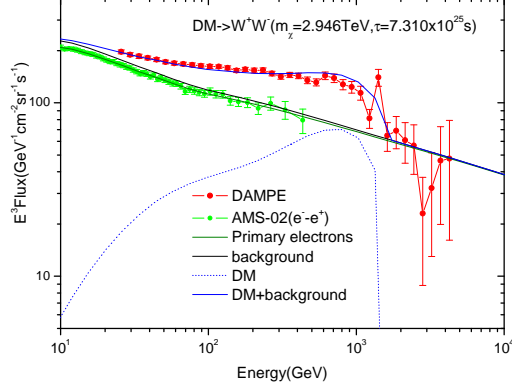


FIG. 3: Spectrum for dark matter decay via the W^+W^- case.

in principle different. Nevertheless, in the end we find that the results are quite similar in our cases. In Fig.3 we show the spectrum of the decay in model A (W^+W^- case). The spectrum is very close to that of the annihilations, though the energy is doubled with $m_\chi = 2.946\text{TeV}$. The life time of the decaying particle is $\tau = 7.31 \times 10^{25}\text{s}$. As the spectrum for the annihilation and decay are quite similar, we shall mainly discuss the annihilations, though most of the results are also applicable to decays.

IV. THE PEAK AND NEARBY SOURCE

In the last section we see that the galactic halo dark matter annihilation could provide a reasonably good fit to the DAMPE e^+e^- spectrum, though it does require a very large annihilation cross section. However, there is no peak produced in the spectrum. Here, we tentatively treat the peak as real, and consider whether such a peak could be produced in dark matter annihilation or decay from a nearby subhalo. To do this, we use the **GALPROP** code to compute the primary background and dark matter contribution from the galactic halo, then adding the contribution from the nearby subhalo. The dark matter parameters and subhalo parameters are varied to fit the DAMPE spectrum.

A. Global Fit Models

First we consider the two models introduced in Sec. II: in model A, in which the e^+e^- are produced by the direct channel and the W^+W^- channel; and model B, in which the e^+e^- production are mainly from the direct channel and the $\tau^+\tau^-$ channels. The branching ratio of the direct channel and the other channels are taken as free parameters.

Model A. In Fig.4, we plot the best fit to the DAMPE spectrum. The CR background, the various contribu-

tions from dark matter annihilations, and the total of these are all plotted in the figure. As we can see from the figure, there is no peak in the total spectrum curve, which behaves as a gentle break, despite the fact that a subhalo is introduced. Looking into the details, we see the W^+W^- channel broad spectrum (i.e. the one from galactic halo annihilations) gives an excellent fit to the broad excess, which are the majority of the data and also have much smaller measurement error bars than the few data points near the 1.4 TeV peak. As a result, the W^+W^- channel is the dominant contribution to the e^+e^- spectrum. The broad e^-e^+ spectrum (i.e. the direct channel contribution from the galactic halo), on the other hand, does not have the correct shape to fit the broad excess, so its contribution must be suppressed. We plot the $f - \log A$ distribution in Fig. 5, with other parameters marginalized. We find that the branching ratio is limit to be $f \lesssim 1.1 \times 10^{-4}$, meaning that the contribution from e^+e^- channel is quite limited compared with the W^+W^- channel. Thus, the whole spectrum shape is determined by the W^+W^- channel. The branching ratio of the direct channel to the W^+W^- channel f is however a single parameter, so the direct e^+e^- from the subhalo which has the desirable spectral shape of a peak is also suppressed. The final spectrum fits most of the data, but does not have a peak, and is not significantly better than the broad spectrum fit given in Sec. II.

Is it possible for the direct e^+e^- channel to dominate over the W^+W^- channel? Unfortunately, for realistic parameters for cosmic ray propagation and dark matter halo, the galactic halo annihilation to direct e^+e^- channel produce fairly hard spectrum, even after the diffusion process, as shown by the cyan colored curve in Fig.4. The curve is broader than that of the nearby subhalo contribution, but still too narrow to produce the broad excess.

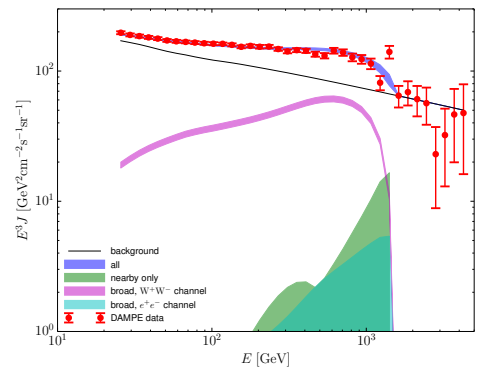


FIG. 4: The fit to DAMPE spectrum with model A, with various contributions shown and marked. The envelope corresponds to 1σ in parameter space.

Model B. In Figs. 6 and 7 we show the corresponding results for model B. In this case, the fitting curve passes closer to the peak point, but the spectral shape is more like a cliff than a peak, the flux on the left side

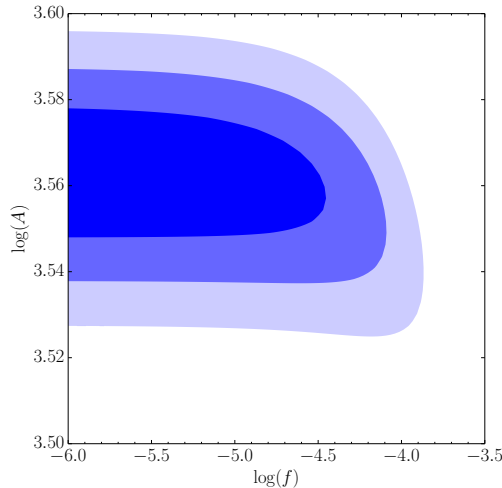
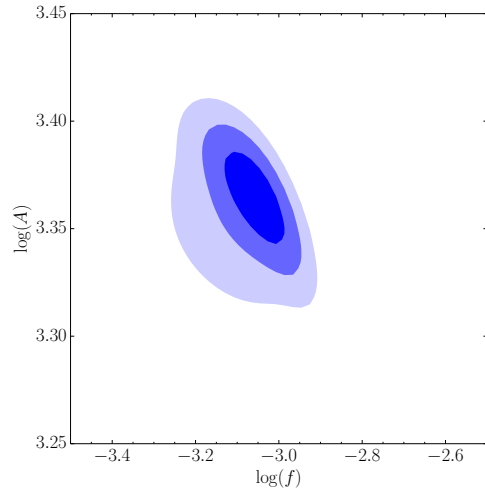
FIG. 5: The constraints on f and A for model A.

FIG. 7: Same as Fig. 5, but for model B.

of the peak is over-predicted. In fact, in this model the main contribution to the 1.4 TeV spectrum is not from the nearby subhalo, but instead from the direct e^+e^- channel component in the broad spectrum, i.e. from the galactic halo dark matter annihilation or decay. Another problem is that the flux at energy around several tens GeVs were under predicted. Though the deviation is not very obvious on this plot, the measurement error in that energy range is much smaller. In this model, we obtain $5.6 \times 10^{-4} \lesssim f \lesssim 1.2 \times 10^{-3}$ at 3σ .

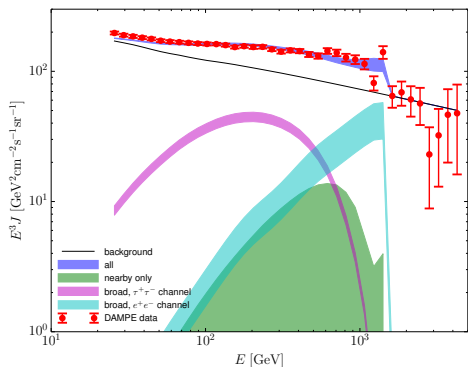


FIG. 6: Same as Fig. 4, but for model B.

In all these global fit models, the contribution from a possible nearby subhalo is limited to $\lesssim 10 - 20\%$. This small contribution is not apparent in the flux, and fails to produce the peak-like feature.

B. Eye Ball Fit Models

In the above we have seen that even with nearby subhalo, the global fit models do not produce a sharp peak in

the spectrum. Here we consider how such a peak might be generated if we relax the requirement on the fit.

The different components have different spectral shapes. The background electrons have a simple power law shape and its normalization is determined by using the positron spectrum measured in the AMS-02 experiment. The direct e^+e^- , W^+W^- and $\tau^+\tau^-$ channels from the galactic halo annihilation also have essentially fixed spectral shape, though it depends on the galactic halo model and the cosmic ray propagation parameters. The normalization of these depends on the dark matter annihilation cross section or decay width. In fact, the shapes are slightly different for the case of annihilation and the case of decay, as the radial profile of production in the galactic halo are different, though we find that the difference is not large. On the other hand, for the nearby components the shape depend on the distance of the subhalo. This change is most obvious for the direct e^+e^- channel, while for the $\tau^+\tau^-$ channel the change is not very significant. By adjusting the branching ratio, one could change the relative contributions of the direct, W^+W^- and $\tau^+\tau^-$ channels, and by adjusting the subhalo distance and mass, one could change the relative contribution from the subhalo and the galactic halo. The various different components are summed up to produce the total spectrum.

We note that the measurement error on the spectrum is smaller at lower energy scales. When performing a global fit with natural weight according to Eq. (9), the low energy part of the spectrum would largely determine the fit, that is the reason why the contribution of the direct e^+e^- component is strongly suppressed in the above, because the shape of broad (i.e. galactic) direct e^+e^- component does not fit the lower energy part of the spectrum. This is also why the W^+W^- component is strongly favored, because its shape agrees extremely well with the observed excess. Here, to study whether a peak feature

can be generated, we will give up the minimal variance fit based on the χ^2 , but use an “eye ball fit” to produce the spectrum. Note that even though the spectrum may appear to the eye to fit the data well, the actual χ^2 value would be much larger than the global fits we obtained above.

In performing the “eye ball fit”, we shall ignore the data above 2 TeV, where a dip appeared in the $E^3\text{Flux}$ plot. In this part the error is too large to draw definite conclusions.

Model A. Since the broad (galactic halo) W^+W^- component has a shape very well suited for fitting the broad excess, we try to produce a spectrum with the broad and nearby (subhalo) W^+W^- components as principal contributions in addition to the background. We have tried various combination of the two, and show one example of such “eye ball fit” in Fig.8. We see the broad W^+W^- has a relatively flat shape up to 0.7 TeV, above which it drops rapidly. By contrast, the nearby W^+W^- source produce a one sided peak at $\sim 1.4\text{TeV}$, it drops to zero above 1.4 TeV, while declines rapidly at smaller energy. If we adjust the relative contribution of the two, we could create a slight hill in the spectrum at the desired position. However, we see that the hill has a gentle slope on the left side, though on the right side it could be very steep. Also, on the low energy part the fit is not too good: it is obviously below the data point. To get a better fit on the low energy part, one has to increase the amplitude of the broad W^+W^- component. This can be achieved by increasing the annihilate cross section or decay width, but then the nearby source component would also increase, increasing the peak height while keep the same shape. If one wants to maintain the height by reducing the nearby source component (this can be done by adjusting the subhalo mass), the relative amplitude of the two components will be changed, and the slope below 1.4 TeV would be even more gentle, making the peak disappear into a one sided slope, which is essentially the result of global best fit of model A above.

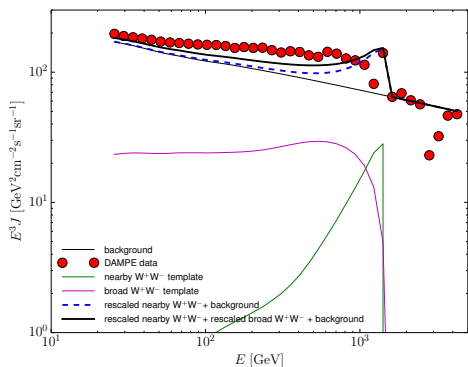


FIG. 8: An eye ball fit to the DAMPE spectrum with principal contribution from the broad and nearby W^+W^- components.

Model B. Next we consider the fit with the direct

e^+e^- channels. The advantage of this channel is that the nearby source of this channel may generate very sharp peak, though its broad component has the wrong shape to fit the broad excess. If we relax the fit to the broad excess though, we could produce a peaked spectrum in this case. The $\tau^+\tau^-$ components which have flatter shapes may also be employed to help improve the fit to the low energy broad excess part. An “eye ball fit” is shown in Fig.9. Here we see the total spectrum (marked as “adjusted spectrum”) can well reproduce the peak feature at 1.4 TeV. This peak feature is dominated by contribution from the nearby direct e^+e^- source. Interestingly, the broad e^+e^- source, the nearby and broad $\tau^+\tau^-$ source together make up the contribution to the broad excess at a few hundred GeVs. Nevertheless, the total spectrum at the few hundred GeVs are still significantly below that of the observation. If one wants to improve the fit to that part from these components, however, one would have to increase the $\tau^+\tau^-$ contribution, which would again make the peak change into a slope or cliff, as the case of global fit model B.

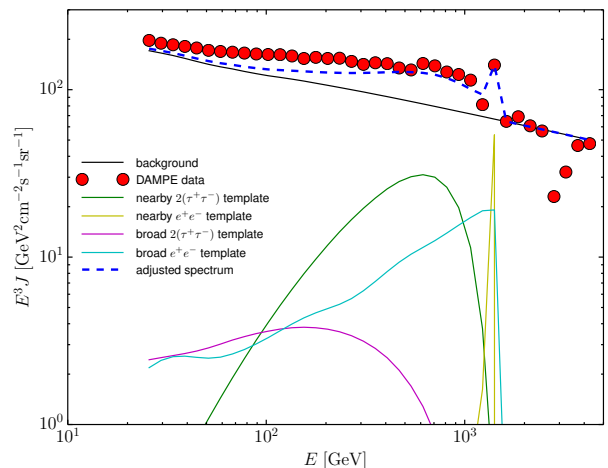


FIG. 9: A model B fit with adjusted background.

C. Rescaled Background Model

In our analysis of the DAMPE data, we distinguish the “background”, which is the part of the spectrum contributed by normal astrophysical sources, and the excess, which we attribute to the contribute of dark matter. In the above we have used the experimentally derived background from the AMS-02 experiment. However, there are uncertainties in such decomposition. Here we consider the some other way of decomposition. To do this, we rescale the background as follows: we rescale the experimentally derived background by a factor $1.13 \times \exp(-E/5\text{TeV})$.

With this change, the fit to the broad excess can be

significantly improved for the model B. We show the fit to the model with the rescaled background in Fig. 10. Here, compared with the global best fit model of the original background, the reduced χ^2 of the best fit model decreased from 2.2 to 0.7. This is because with the adjusted background, the shape of the $\tau^+\tau^-$ components have much better match with the broad excess. The best fit model still does not show the narrow peak, but a model with the narrow peak is only slightly worse fit to the model than the best fit one. See the green dashed line in Fig. 10.

This example shows that we have to view the various fits with some caution. Systematic uncertainty such as the definition of the background could be very important in our interpretation of the data.

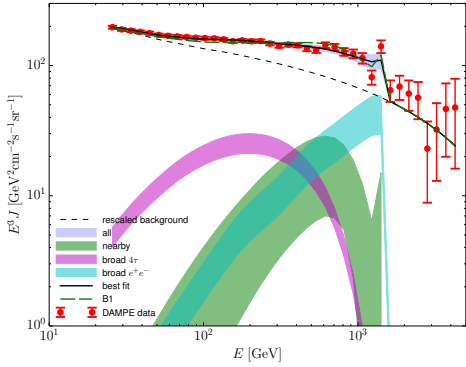


FIG. 10: A fit to the DAMPE spectrum with adjusted background, for the e^+e^- and double $\tau^+\tau^-$ channels.

V. THE SUBHALO

We now consider the subhalo which can produce the peak shown above. We let the electrons and positron of a subhalo plus the background fit the points near the peak.

A. Decaying dark matter subhalo

For decaying dark matter with mass $m_\chi = 2E_0/c^2$, and the lifetime t_χ , the injection rate is

$$Q_{\text{decay}} = \frac{2M_{\text{sub}}}{m_\chi t_\chi} = \frac{M_{\text{sub}}}{E_0/c^2 t_\chi} = 2.6 \times 10^{39} \frac{M_{\text{sub}}}{E_0 t_\chi} \text{ s}^{-1}, \quad (11)$$

where M_{sub} is subhalo mass in units of solar mass, E_0 in units GeV and t_χ in units Universe age (4.4×10^{17} s). If we adopt the life time value $t_\chi = 7.31 \times 10^{25} \text{ s}^{-1}$, in which the galactic halo contribution could produce the broad process, the result is shown on Fig. 11.

We see that for a reasonable distance of 0.1 kpc, the required halo mass is about $10^9 M_\odot$. Such a heavy subhalo would create large gravitational perturbation on galactic

disc which could hardly escape the notice of astronomers. Increasing the decay rate would greatly raise the galactic halo contribution to a level above the broad excess. We conclude that the 1.4 TeV peak can not be explained by dark matter decay.

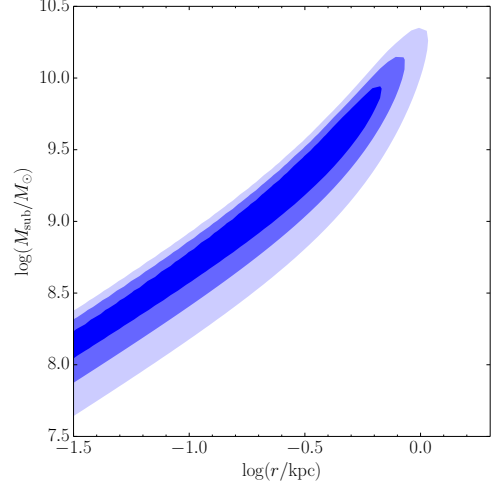


FIG. 11: The constraints on the $\log(r) - \log(M_{\text{sub}})$ by fitting only the peak for decaying dark matter.

B. Annihilating dark matter subhalo

For dark matter annihilation, the density profile of the subhalo is crucial. For the subhalo, we assume a power-law density profile (e.g. [62–64])

$$\rho(r) = \rho_0 r^{-\alpha}, \quad M_{\text{sub}} = \frac{4\pi\rho_0}{3-\alpha} r_t^{3-\alpha}, \quad (12)$$

where r_t is the tidal radius, and

$$\rho_0 = \frac{(3-\alpha)M_{\text{sub}}}{4\pi r_t^{3-\alpha}} \quad (13)$$

The inner cutoff radius for cuspy halo is determined by equating the annihilation time scale to dynamical time scale, $\tau_d = \tau_{\text{anni}}$, where

$$\tau_d = \frac{r_t}{\sqrt{GM_{\text{sub}}/r_t}}, \quad \tau_{\text{anni}} = \frac{n_\chi(r_c)}{\dot{n}_\chi(r_c)}. \quad (14)$$

Finally the injection rate from the annihilating dark matter in the subhalo is given by

$$Q_{\text{anni}} = \int_{r_c}^{r_t} 2 \left(\frac{\rho_0 c^2}{E_0} r^{-\alpha} \right)^2 \langle \sigma v \rangle 4\pi r^2 dr \quad (15)$$

$$= \begin{cases} 8\pi \left(\frac{\rho_0 c^2}{E_0} \right)^2 \langle \sigma v \rangle \frac{(r_t^{3-2\alpha} - r_c^{3-2\alpha})}{3-2\alpha} & \text{when } \alpha \neq 1.5 \\ 8\pi \left(\frac{\rho_0 c^2}{E_0} \right)^2 \langle \sigma v \rangle [\ln(r_t) - \ln(r_c)] & \text{when } \alpha = 1.5. \end{cases}$$

For annihilation we assume $\langle\sigma v\rangle \approx 10^{-23}\text{cm}^3\text{s}^{-1}$, for which the annihilation of the galactic halo gives the broad excess. Then, if the peak is due to the subhalo, the mass and distance of the subhalo is shown in Fig. 12. To fit the peak, assuming the subhalo is located at ~ 0.1 kpc from the Solar system, the required subhalo mass is $\sim 10^6 - 10^8 M_\odot$ for $\alpha = 1.5$, which is still quite significant. If the halo has a steeper profile, e.g. $\alpha = 2.0$, then the halo mass could be as small as $\sim 3 \times 10^3 - 1.5 \times 10^4 M_\odot$. Thus, we see that to produce the 1.4 TeV peak from annihilations in the peak, we need either a relatively heavy subhalo, or a smaller one if it has a very steep density profile, which may be generated by e.g. accretion of primordial black holes [65–67]

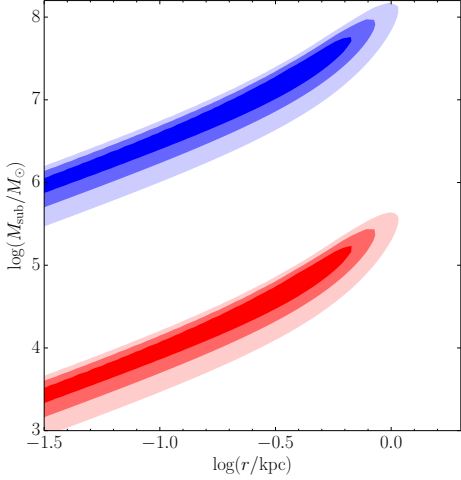


FIG. 12: The constraints on the $\log(r)$ - $\log(M_{\text{sub}})$ for dark matter annihilation case, $\langle\sigma v\rangle = 1 \times 10^{-23}$ is assumed. The blue contours for $\alpha = 1.7$, red for $\alpha = 2$.

C. Inverse Compton Scattering

If such a subhalo is located near the Solar system, it might also produce strong γ -ray photons. Even if we conservatively assume that photons are not produced in the decay or annihilation, the electrons and positrons produced by the subhalo would have inverse Compton scattering (ICS) with background photons. If a subhalo is a strong electrons/positrons source, it is also a strong ICS source. This would help to identify the subhalo by looking for nearby bright and somewhat extended gamma-ray sources.

The emissivity of the up scattered photons is [68]

$$\epsilon(\mathcal{E}, E_0, Q, r) = \int dE \frac{\psi}{4\pi} \int d\mathcal{E}_0 \frac{3\sigma_T c}{4\gamma^2 \mathcal{E}_0} G(q, \Gamma_e) \frac{dU_{\text{rad}}}{\mathcal{E}_0 d\mathcal{E}_0} \quad (16)$$

where ψ is from Eq. 7, \mathcal{E}_0 and \mathcal{E} are the energy of photons before and after scattering, $dn/d\mathcal{E}_0$ is the number density

of photons per unit energy for the interstellar radiation field.

$$\Gamma_e = \frac{4\mathcal{E}_0\gamma}{m_e c^2}, \quad q = \frac{\mathcal{E}}{(\gamma m_e c^2 - \mathcal{E})\Gamma_e}, \quad (17)$$

and the function

$$G(q, \Gamma_e) = 2q \ln q + (1 + 2q)(1 - q) + \frac{(\Gamma_e q)^2 (1 - q)}{2(1 + \Gamma_e q)}. \quad (18)$$

From [69, 70], near our Sun, the interstellar radiation field has three peaks at the NIR ($\sim 1\mu\text{m}$), FIR ($\sim 100\mu\text{m}$) and CMB ($\sim 1000\mu\text{m}$), with energy density $\sim 0.4 \text{ eV cm}^{-3}$, $\sim 0.3 \text{ eV cm}^{-3}$ and $\sim 0.2 \text{ eV cm}^{-3}$ respectively. Adopting these values we have

$$\epsilon(\mathcal{E}, E_0, Q, r) \approx \frac{1}{4\pi} \int dE \psi \sum_i \frac{3\sigma_T c U_{\text{rad},i}}{4\gamma^2 \mathcal{E}_{0,i}^2} G(q_i, \Gamma_{e,i}) \quad (19)$$

where i is one of NIR, FIR or CMB respectively.

If the line-of-sight is θ offset from the center of the subhalo, we have the specific intensity of photons up scattered by electrons generated from a source with Q injection rate and distance r from the observer,

$$I_\theta(\mathcal{E}, E_0, Q, r, \theta) = \int_0^\infty \epsilon(\mathcal{E}, E_0, Q, x') dr', \quad (20)$$

where $x' = \sqrt{r^2 + r'^2 - 2rr'\cos\theta}$.

We show the ICS specific intensity at 30 GeV for line-of-sight toward the center of the subhalo in Fig. 13. It is well above the isotropic gamma radiation background (IGRB) given in [71]. Such a source should in principle be observable with the γ -ray telescope such as Fermi and DAMPE, though as an extended source extracting it from the various background and foreground sources may not be trivial. Also interesting is that the expected flux decreases with decreasing distance, this is because to achieve the DAMPE peak, the more nearby source needs to produce fewer number of electrons, hence also generating less ICS radiation.

D. Anisotropy

Finally, we note that if the nearby subhalo is invoked, it may generate a large anisotropy in the CR flux. The amplitude of the dipole anisotropy is (Globus2017)

$$\left(\frac{\delta J}{J}\right)_{\text{max}} \sim \frac{3D_{xx}}{c\psi} \left|\frac{d\psi}{dr}\right|, \quad (21)$$

If we require $\delta J/J \lesssim 1$, i.e. without generating obvious anisotropy in the cosmic ray flux, we find that the subhalo $r \lesssim 0.03\text{kpc}$ can be excluded.

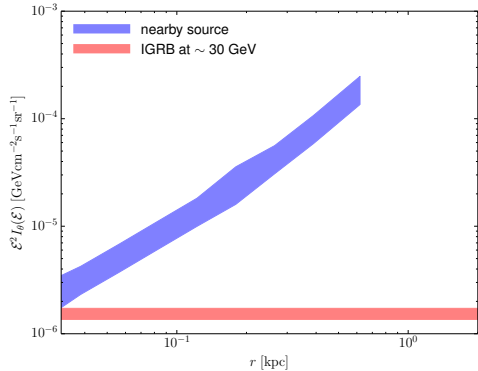


FIG. 13: The predicted gamma-ray intensity at 30 GeV for a subhalo with electrons/positrons that fits the peak (with 1σ C.L.), for line-of-sight toward the subhalo center. In the panel we also plot the IGRB given by paper [71].

VI. SUMMARY

We studied the CR electron and positron spectrum from dark matter annihilation or decay in the energy range of the recent DAMPE measurement. We extracted the broad excess in the spectrum from a few tens GeV to about 2 TeV, by using the AMS-02 data on positron spectrum. We then derive the electron and positron spectrum using the CR propagation model. We find that for both the W^+W^- channel and the combination of direct e^+e^- and double $\tau^+\tau^-$ channels, dark matter annihilation or decay in the galactic halo can provide good fits to the broad excess in the e^+e^- spectrum, or double the mass for decays to particle pairs. This naturally explains the TeV break found in the CR e^+e^- spectrum. However, this requires a cross section of $\langle\sigma v\rangle \sim 10^{-23}\text{cm}^3\text{s}^{-1}$, which is larger than the WIMP cross section required for obtaining the correct dark matter abundance through thermal decoupling in the early universe.

In the DAMPE spectrum, there is also a prominent single point peak at 1.4 TeV. Tentatively treating it as real, we investigate how such a peak could be produced, despite the energy loss while the electrons and positrons diffusing through the interstellar space. We consider the possibility that the peak is produced by a nearby dark matter subhalo. We find that in the global fit models, there is no peak in the spectrum, and inclusion of the

nearby subhalo does not significantly improve the fit. This is because to match the shape of broad spectrum, a suppressed contribution from the e^+e^- channel is favored by the data. As a result, a nearby subhalo is hard to generate a narrow peak, as spectrum of electrons and positrons generated by other channels are always broad.

We then relaxed the requirement of fitting the whole spectrum data, and studied how a spectrum with a 1.4 TeV peak could be generated. We find that in the case of W^+W^- channel, a peak feature with gentle slope on the low energy side and steep slope on the high energy side can be produced. In the case of direct e^+e^- channel and double $\tau^+\tau^-$ channel, a sharp peak feature as found in the DAMPE data could be produced. However, in these cases, the fitting to the broad excess from a few tens to a few hundred GeVs are not very good. In these fits, however, we have assumed a background derived from the AMS-02 experiment. If we rescale this background, a better fit can be obtained for the double $\tau^+\tau^-$ channel, even with a peak. These show that the precisely measured spectral shape from DAMPE could provide stringent constraint on the model, though theoretical uncertainty is a very important factor in making interpretation and obtaining the constraint.

Giving the peak strength, we estimate the mass and distance of the subhalo. We find the halo is very heavy ($\sim 10^9 M_\odot$ for the decaying dark matter model, if we assume this is also the source for broad excess. In the case of annihilations, the mass of the subhalo is also relatively large ($\sim 10^6 M_\odot$), though it depends on the density profile and for very steep profile $\alpha = 2$, reasonable mass could be obtained. We also considered the inverse Compton scattering by the electrons, which may produce observable γ -ray radiation, and the anisotropy in cosmic ray if the subhalo is too close by.

Acknowledgments

We thank Prof. Jin Chang and Dr. Xiaoyuan Huang for helpful discussions. XLC acknowledges the support of the the NSFC through grant No. 1633004 and 11373030, the MoST through grant 2016YFE0100300, and the CAS Frontier Science Key Project No. QYZDJ-SSW-SLH017. BY acknowledges the support of Bairen program from the Chinese Academy of Sciences (CAS).

[1] Planck Collaboration, P. A. R. Ade, N. Aghanim, M. Arnaud, M. Ashdown, J. Aumont, C. Baccigalupi, A. J. Banday, R. B. Barreiro, J. G. Bartlett, et al., *A&A* **594**, A13 (2016), 1502.01589.
 [2] M. Battaglieri, A. Belloni, A. Chou, P. Cushman, B. Echenard, R. Essig, J. Estrada, J. L. Feng, B. Flaugher, P. J. Fox, et al., *ArXiv e-prints* (2017), 1707.04591.

[3] A. W. Strong, I. V. Moskalenko, and V. S. Ptuskin, *Annual Review of Nuclear and Particle Science* **57**, 285 (2007), astro-ph/0701517.
 [4] M. A. DuVernois, S. W. Barwick, J. J. Beatty, A. Bhattacharyya, C. R. Bower, C. J. Chaput, S. Coutu, G. A. de Nolfo, D. M. Lowder, S. McKee, et al., *ApJ* **559**, 296 (2001).
 [5] J. Chang, J. H. Adams, H. S. Ahn, G. L.

- Bashindzhagyan, M. Christl, O. Ganel, T. G. Guzik, J. Isbert, K. C. Kim, E. N. Kuznetsov, et al., *Nature* **456**, 362 (2008).
- [6] O. Adriani, G. C. Barbarino, G. A. Bazilevskaya, R. Bellotti, M. Boezio, E. A. Bogomolov, M. Bongi, V. Bonvicini, S. Borisov, S. Bottai, et al., *Physical Review Letters* **106**, 201101 (2011), 1103.2880.
- [7] A. A. Abdo, M. Ackermann, M. Ajello, W. B. Atwood, M. Axelsson, L. Baldini, J. Ballet, G. Barbiellini, D. Bastieri, M. Battelino, et al., *Physical Review Letters* **102**, 181101 (2009), 0905.0025.
- [8] S. Abdollahi, M. Ackermann, M. Ajello, W. B. Atwood, L. Baldini, G. Barbiellini, D. Bastieri, R. Bellazzini, E. D. Bloom, R. Bonino, et al., *Phys. Rev. D* **95**, 082007 (2017).
- [9] M. Aguilar, D. Aisa, B. Alpat, A. Alvino, G. Ambrosi, K. Andeen, L. Arruda, N. Attig, P. Azzarello, A. Bachlechner, et al., *Physical Review Letters* **113**, 221102 (2014).
- [10] A. Abramowski, F. Acero, F. Aharonian, A. G. Akhperjanian, G. Anton, A. Barnacka, U. Barres de Almeida, A. R. Bazer-Bachi, Y. Becherini, J. Becker, et al., *Physical Review Letters* **106**, 161301 (2011), 1103.3266.
- [11] F. Aharonian, A. G. Akhperjanian, U. Barres de Almeida, A. R. Bazer-Bachi, Y. Becherini, B. Behera, W. Benbow, K. Bernlöhner, C. Boisson, A. Bochow, et al., *Physical Review Letters* **101**, 261104 (2008), 0811.3894.
- [12] F. Aharonian, A. G. Akhperjanian, G. Anton, U. Barres de Almeida, A. R. Bazer-Bachi, Y. Becherini, B. Behera, K. Bernlöhner, A. Bochow, C. Boisson, et al., *A&A* **508**, 561 (2009), 0905.0105.
- [13] L. Bergström, J. Edsjö, and G. Zaharijas, *Physical Review Letters* **103**, 031103 (2009), 0905.0333.
- [14] J. L. Feng, M. Kaplinghat, and H.-B. Yu, *Phys. Rev. D* **82**, 083525 (2010), 1005.4678.
- [15] G. Zaharijas, A. Cuoco, Z. Yang, J. Conrad, and for the Fermi-LAT collaboration, *ArXiv e-prints* (2010), 1012.0588.
- [16] Y. Zhao, X.-J. Bi, H.-Y. Jia, P.-F. Yin, and F.-R. Zhu, *Phys. Rev. D* **93**, 083513 (2016), 1601.02181.
- [17] W. Liu, X.-J. Bi, S.-J. Lin, B.-B. Wang, and P.-F. Yin, *Phys. Rev. D* **96**, 023006 (2017), 1611.09118.
- [18] B.-Q. Lu, Y.-L. Wu, W.-H. Zhang, and Y.-F. Zhou, *ArXiv e-prints* (2017), 1711.00749.
- [19] Y. Zhao, X.-J. Bi, P.-F. Yin, and X. Zhang, *ArXiv e-prints* (2017), 1711.04696.
- [20] S.-J. Lin, Q. Yuan, and X.-J. Bi, *Phys. Rev. D* **91**, 063508 (2015), 1409.6248.
- [21] D. Malyshev, I. Cholis, and J. Gelfand, *Phys. Rev. D* **80**, 063005 (2009), 0903.1310.
- [22] H.-B. Hu, Q. Yuan, B. Wang, C. Fan, J.-L. Zhang, and X.-J. Bi, *ApJ* **700**, L170 (2009), 0901.1520.
- [23] I. Cholis and D. Hooper, *Phys. Rev. D* **88**, 023013 (2013), 1304.1840.
- [24] R. Blandford, P. Simeon, and Y. Yuan, *Nuclear Physics B Proceedings Supplements* **256**, 9 (2014), 1409.2589.
- [25] J. Chang, G. Ambrosi, Q. An, R. Asfandiyarov, P. Azzarello, P. Bernardini, B. Bertucci, M. S. Cai, M. Caragiulo, D. Y. Chen, et al., *Astroparticle Physics* **95**, 6 (2017), 1706.08453.
- [26] DAMPE collaboration, *Nature* **551** (2017), arxiv:1711.10981.
- [27] V. S. Berezhinskii, S. V. Bulanov, V. A. Dogiel, and V. L. Ginzburg, *Astrophysics of cosmic rays* (North-Holland, Amsterdam, 1990), ISBN 0444886419.
- [28] A. W. Strong and I. V. Moskalenko, *The Astrophysical Journal* **509**, 212 (1998), ISSN 0004-637X, 9807150, URL <http://arxiv.org/abs/astro-ph/9807150><http://stacks.iop.org/0004-637X/509/i=1/a=212>.
- [29] R. Blandford and D. Eichler, *Physics Reports* **154**, 1 (1987), ISSN 03701573, URL <http://linkinghub.elsevier.com/retrieve/pii/0370157387901347>.
- [30] A. E. Vladimirov, S. W. Digel, G. Jóhannesson, P. F. Michelson, I. V. Moskalenko, P. L. Nolan, E. Orlando, T. A. Porter, and A. W. Strong, *Computer Physics Communications* **182**, 1156 (2011), 1008.3642.
- [31] I. V. Moskalenko, A. W. Strong, J. F. Ormes, and M. S. Potgieter, *The Astrophysical Journal* **565**, 280 (2001), ISSN 0004-637X, 0106567, URL <http://stacks.iop.org/0004-637X/565/i=1/a=280><http://arxiv.org/abs/astro-ph/0106567><http://dx.doi.org/10.1086/324402>.
- [32] A. Strong and J. Mattox, *Astron. Astrophys.* **308**, L21 (1996).
- [33] M. Aguilar, D. Aisa, B. Alpat, A. Alvino, G. Ambrosi, K. Andeen, L. Arruda, N. Attig, P. Azzarello, A. Bachlechner, et al., *Physical Review Letters* **114**, 171103 (2015), ISSN 0031-9007, URL <http://link.aps.org/doi/10.1103/PhysRevLett.114.171103>.
- [34] M. Aguilar, L. Ali Cavazonza, G. Ambrosi, L. Arruda, N. Attig, S. Aupetit, P. Azzarello, A. Bachlechner, F. Barao, A. Barrau, et al., *Physical Review Letters* **117**, 231102 (2016), ISSN 0031-9007, URL <http://link.aps.org/doi/10.1103/PhysRevLett.117.231102>.
- [35] H.-B. Jin, Y.-L. Wu, and Y.-F. Zhou, *Journal of Cosmology and Astroparticle Physics* **2015**, 049 (2015), ISSN 1475-7516, 1410.0171, URL <http://arxiv.org/abs/1410.0171><http://dx.doi.org/10.1088/1475-7516/2015/09/049><http://stacks.iop.org/1475-7516/2015/i=09/a=049?key=crossref.cf4074bcdab63e1efbd17a2b3ed849a9>.
- [36] J. F. Navarro, C. S. Frenk, and S. D. M. White, *The Astrophysical Journal* **490**, 493 (1996), ISSN 0004-637X, 9611107, URL <http://stacks.iop.org/0004-637X/490/i=2/a=493><http://arxiv.org/abs/astro-ph/9611107>.
- [37] L. Bergstrom, P. Ullio, and J. Buckley, *Astroparticle Physics* **9**, 44 (1997), ISSN 09276505, 9712318, URL <http://linkinghub.elsevier.com/retrieve/pii/S0927650598000152><http://arxiv.org/abs/astro-ph/9712318>.
- [38] B. Moore, S. Ghigna, F. Governato, G. Lake, T. Quinn, J. Stadel, and P. Tozzi, *The Astrophysical Journal* **524**, 4 (1999), ISSN 0004637X, 9907411, URL <http://stacks.iop.org/1538-4357/524/i=1/a=L19><http://arxiv.org/abs/astro-ph/9907411>.
- [39] J. Einasto, in *Astronomy and Astrophysics 2010* (2009), p. 31, 0901.0632, URL <http://inspirehep.net/record/810367/files/arXiv:0901.0632.pdf><http://arxiv.org/abs/0901.0632>.
- [40] T. Sjöstrand, S. Mrenna, and P. Skands, *Computer Physics Communications* **178**, 852 (2008), ISSN 00104655, 0710.3820.
- [41] H.-B. Jin, Y.-L. Wu, and Y.-F. Zhou (2017), 1701.02213, URL <http://arxiv.org/abs/1701.02213>.
- [42] M. Aguilar, D. Aisa, A. Alvino, G. Ambrosi, K. Andeen, L. Arruda, N. Attig, P. Azzarello, A. Bachlechner, F. Barao, et al., *Physical Review Letters* **113**, 121102

- (2014), ISSN 0031-9007, URL <http://link.aps.org/doi/10.1103/PhysRevLett.113.121102>.
- [43] L. Accardo, M. Aguilar, D. Aisa, B. Alpat, A. Alvino, G. Ambrosi, K. Andeen, L. Arruda, N. Attig, P. Azarello, et al., Physical Review Letters **113**, 121101 (2014), ISSN 0031-9007, URL <http://link.aps.org/doi/10.1103/PhysRevLett.113.121101>.
- [44] H.-B. Jin, Y.-L. Wu, and Y.-F. Zhou, Journal of Cosmology and Astroparticle Physics **2013**, 026 (2013), ISSN 1475-7516, 1304.1997, URL <http://arxiv.org/abs/1304.1997><http://stacks.iop.org/1475-7516/2013/i=11/a=026?key=crossref.f20a7d57bb9d81eb2e16a956852d6257>.
- [45] Z.-P. Liu, Y.-L. Wu, and Y.-F. Zhou, Physical Review D **88**, 096008 (2013), ISSN 1550-7998, 1305.5438, URL <http://link.aps.org/doi/10.1103/PhysRevD.88.096008><http://arxiv.org/abs/1305.5438><http://dx.doi.org/10.1103/PhysRevD.88.096008>.
- [46] J. Chen, Z.-L. Liang, Y.-L. Wu, and Y.-F. Zhou, Journal of Cosmology and Astroparticle Physics **2015**, 021 (2015), ISSN 1475-7516, 1505.04031, URL <http://stacks.iop.org/1475-7516/2015/i=12/a=021?key=crossref.b908c4fbd5e06fa301b2247a48fd09b3><http://arxiv.org/abs/1505.04031><http://dx.doi.org/10.1088/1475-7516/2015/12/021>.
- [47] Y.-F. Zhou, PoS **DSU2015**, 22 (2016).
- [48] D. Chen, J. Huang, and H.-B. Jin, The Astrophysical Journal **811**, 154 (2015), ISSN 1538-4357, 1412.2499, URL <http://arxiv.org/abs/1412.2499><http://stacks.iop.org/0004-637X/811/i=2/a=154?key=crossref.3e1ffab3e9880c2872c472c1e008a3f2>.
- [49] P. Salucci, F. Nesti, G. Gentile, and C. F. Martins, Astronomy & Astrophysics **523**, 6 (2010), ISSN 0004-6361, 1003.3101, URL <http://www.aanda.org/10.1051/0004-6361/201014385><http://arxiv.org/abs/1003.3101>.
- [50] A. W. Strong, I. V. Moskalenko, and O. Reimer, The Astrophysical Journal **537**, 763 (2000), ISSN 0004-637X, 9811296, URL <http://arxiv.org/abs/astro-ph/9811296><http://stacks.iop.org/0004-637X/537/i=2/a=763>.
- [51] B. Moore, S. Ghigna, F. Governato, G. Lake, T. Quinn, J. Stadel, and P. Tozzi, ApJ **524**, L19 (1999), astro-ph/9907411.
- [52] A. Klypin, A. V. Kravtsov, O. Valenzuela, and F. Prada, ApJ **522**, 82 (1999), astro-ph/9901240.
- [53] J. S. Bullock and M. Boylan-Kolchin, ARA&A **55**, 343 (2017), 1707.04256.
- [54] R. Trotta, G. Jóhannesson, I. V. Moskalenko, T. A. Porter, R. Ruiz de Austri, and A. W. Strong, ApJ **729**, 106 (2011), 1011.0037.
- [55] D. Staszak and f. t. V. Collaboration, in *Proceedings, 34th International Cosmic Ray Conference (ICRC 2015)* (2015), 1508.06597, URL <https://inspirehep.net/record/1389840/files/arXiv:1508.06597.pdf><http://arxiv.org/abs/1508.06597>.
- [56] F. Aharonian et al. (H.E.S.S.), Phys. Rev. Lett. **101**, 261104 (2008), 0811.3894.
- [57] F. Aharonian et al. (H.E.S.S.), Astron. Astrophys. **508**, 561 (2009), 0905.0105.
- [58] F.-L. Collaboration, :, S. Abdollahi, M. Ackermann, M. Ajello, W. B. Atwood, L. Baldini, G. Barbiellini, D. Bastieri, R. Bellazzini, et al., Physical Review D **95**, 082007 (2017), ISSN 2470-0010, 1704.07195, URL <http://link.aps.org/doi/10.1103/PhysRevD.95.082007><http://arxiv.org/abs/1704.07195><http://dx.doi.org/10.1103/PhysRevD.95.082007>.
- [59] M. Ackermann, M. Ajello, W. B. Atwood, L. Baldini, J. Ballet, G. Barbiellini, D. Bastieri, B. M. Baughman, K. Bechtol, F. Bellardi, et al., Physical Review D **82**, 092004 (2010), ISSN 1550-7998, 1008.3999, URL <http://link.aps.org/doi/10.1103/PhysRevD.82.092004>.
- [60] VERITAS Collaboration, S. Archambault, A. Archer, W. Benbow, R. Bird, E. Bourbeau, T. Brantseg, M. Buchovecky, J. H. Buckley, V. Bugaev, et al., Physical Review D **95**, 082001 (2017), ISSN 2470-0010, 1703.04937, URL <http://link.aps.org/doi/10.1103/PhysRevD.95.082001><http://arxiv.org/abs/1703.04937><http://dx.doi.org/10.1103/PhysRevD.95.082001>.
- [61] F.-L. Collaboration, Physical Review Letters **115**, 231301 (2015), ISSN 0031-9007, 1503.02641, URL <http://arxiv.org/abs/1503.02641><http://dx.doi.org/10.1103/PhysRevLett.115.231301><http://link.aps.org/doi/10.1103/PhysRevLett.115.231301>.
- [62] D. Reed, F. Governato, L. Verde, J. Gardner, T. Quinn, J. Stadel, D. Merritt, and G. Lake, MNRAS **357**, 82 (2005), astro-ph/0312544.
- [63] J. Diemand, M. Kuhlen, and P. Madau, ApJ **649**, 1 (2006), astro-ph/0603250.
- [64] D. Hooper and S. J. Witte, J. Cosmology Astropart. Phys. **4**, 018 (2017), 1610.07587.
- [65] Y. Yang, European Physical Journal Plus **131**, 432 (2016), 1612.06559.
- [66] Y. Yang, G. Yang, X. Huang, X. Chen, T. Lu, and H. Zong, Phys. Rev. D **87**, 083519 (2013), 1206.3750.
- [67] Y. Yang, G. Yang, and H. Zong, Phys. Rev. D **87**, 103525 (2013), 1305.4213.
- [68] E. Lefa, S. R. Kelner, and F. A. Aharonian, ApJ **753**, 176 (2012), 1205.2929.
- [69] T. A. Porter and A. W. Strong, International Cosmic Ray Conference **4**, 77 (2005), astro-ph/0507119.
- [70] T. A. Porter, I. V. Moskalenko, and A. W. Strong, ApJ **648**, L29 (2006), astro-ph/0607344.
- [71] M. Ackermann, M. Ajello, A. Albert, W. B. Atwood, L. Baldini, J. Ballet, G. Barbiellini, D. Bastieri, K. Bechtol, R. Bellazzini, et al., The Astrophysical Journal **799**, 86 (2015), ISSN 1538-4357, 1410.3696, URL <http://arxiv.org/abs/1410.3696><http://dx.doi.org/10.1088/0004-637X/799/1/86><http://stacks.iop.org/0004-637X/799/i=1/a=86?key=crossref.a653883b23f35ed4242f736b0cff11a5>.